HHS Public Access

Author manuscript

Dev Biol. Author manuscript; available in PMC 2015 November 17.

Published in final edited form as:

Dev Biol. 2008 March 15; 315(2): 317–330. doi:10.1016/j.ydbio.2007.12.038.

Retinoic Acid Regulation of the Mesp-Ripply feedback loop during Vertebrate Segmental Patterning

Tanya A. Moreno, **Roberto Jappelli**, **Juan Carlos Izpisúa Belmonte**, and **Chris Kintner***

The Salk Institute for Biological Studies, 10010 North Torrey Pines Road, La Jolla, CA 92037

Abstract

The *Mesp* bHLH genes play a conserved role during segmental patterning of the mesoderm in the vertebrate embryo by specifying segmental boundaries and anteroposterior (A-P) segmental polarity. Here we use a xenotransgenic approach to compare the transcriptional enhancers that drive expression of the *Mesp* genes within segments of the presomitic mesoderm (PSM) of different vertebrate species. We find that the genomic sequences upstream of the *mespb* gene in the pufferfish *Takifugu rubripes* (*Tr-mespb*) are able to drive segmental expression in transgenic *Xenopus* embryos while those from the *Xenopus laevis mespb* (*Xl-mespb)* gene drive segmental expression in transgenic zebrafish. In both cases, the anterior segmental boundary of transgene expression closely matches the expression of the endogenous *Mesp* genes, indicating that many inputs into segmental gene expression are highly conserved. By contrast, we find that direct retinoic acid (RA) regulation of endogenous *Mesp* gene expression is variable amongst vertebrate species. Both *Tr-mespb* and *Xl-mespb* are directly upregulated by RA, through a complex, distal element. By contrast, RA represses the zebrafish *Mesp* genes. We show that this repression is mediated, in part, by RA-mediated activation of the *Ripply* genes, which together with *Mesp* genes form an RA-responsive negative feedback loop. These observations suggest that variations in a direct response to RA input may allow for changes in A-P patterning of the segments in different vertebrate species.

INTRODUCTION

Many of the segmental features of the vertebrate body plan arise during development by subdivision of the mesoderm into somites. These metameric structures underlie the segmentation of the axial skeleton and musculature, as well as the branching of spinal nerves (Brand-Saberi and Christ, 2000; Christ et al., 2000). Somite formation follows segmental patterning of the mesoderm, a dynamic process that has been extensively studied in mouse, chick, zebrafish and frog embryos. Based on these studies, it has been shown that many of the mechanisms required for segmental patterning are largely conserved, as would be expected for a process that is central to the vertebrate body plan. At the same time, however, slight variations of segmental patterning are likely to be a source of species variation. For

*kintner@salk.edu, (858) 453-4100 x1393.

example, vertebrates vary widely in terms of somite number, size, and morphology. The mechanistic differences that underlie these variations are an essential aspect of segmentation that currently is not well understood.

Key conserved players in the process of segmental patterning in vertebrates are the Mesp bHLH proteins (Buchberger et al., 2002, Sparrow et al., 1998; Buchberger et al., 1998; Saga et al., 1996; Saga et al., 1997; Sawada et al., 2000). *Mesp* genes in mouse, frog, chick and zebrafish are expressed in a similar manner in the anterior presomitic mesoderm (PSM), in a dynamic stripe pattern that is thought to contribute to segmental patterning in several ways. A sharp boundary of *Mesp* gene expression at the anterior edge of a forming segment sets the boundary between one segment and the next, in part by regulating the expression of components in the Eph signaling pathway (Nakajima et al., 2006). In addition, expression of the *Mesp* genes in the anterior half segment is thought to pattern the segment along its A-P axis, with important consequences for subsequent contributions of the anterior and posterior somite halves to the axial skeleton and musculature (e.g. Hrabe de Angelis et al., 1997; Morimoto et al., 2007; Saga et al., 1997). A variety of experiments have shown that perturbing the segmental expression of the *Mesp* genes, even subtly, alters both boundary formation and somitic A-P pattern (Moreno and Kintner, 2004; Morimoto et al., 2006; Morimoto et al., 2007; Morimoto et al., 2005; Nomura-Kitabayashi et al., 2002; Saga, 1998; Saga et al., 1997; Sawada et al., 2000; Sparrow et al., 1998; Takahashi et al., 2003; Takahashi et al., 2005; Takahashi et al., 2007). Thus, a key step in the process of segmental patterning is to establish the proper domains of *Mesp* gene expression within the PSM.

Several factors are known to control segmental gene expression during pattern formation. Activation of *Mesp* expression in the PSM is controlled by a ‘differentiation wavefront’ in which cells in the posterior PSM (the tailbud (TBD); see Fig. 1M) are maintained in an undifferentiated state by FGF8 signaling (Dubrulle et al., 2001; Dubrulle and Pourquie, 2004; Sawada et al., 2001). As cells move anteriorly and escape this signaling, they enter a transition zone (TZ) where they initiate segmental differentiation and upregulate the expression of the *Mesp* genes. Coupled to the passage of the differentiation wavefront is a synchronized oscillation in the Notch pathway that underlies the so-called ‘segmental clock’ (Aulehla and Herrmann, 2004; Cooke and Zeeman, 1976; Dubrulle and Pourquie, 2002; Gridley, 2006; Pourquie, 2001; Saga and Takeda, 2001). The output of this clock contributes by an unknown mechanism to the segmental expression of the *Mesp* genes in the transition zone, perhaps ensuring a sharp boundary of expression between one segment and the next. As the segmental pattern becomes fixed (somitomere region; see Fig. 1M), additional interactions between the *Mesp* genes and the Notch pathway refine the expression of the *Mesp* genes further, thus contributing to the subdivision of the segment into anterior and posterior halves. Finally, *Mesp* gene expression is rapidly extinguished prior to somite formation, through repression mediated by *Ripply* co-repressors (Chan et al., 2006; Kawamura et al., 2005; Kondow et al., 2006; Morimoto et al., 2007). Mesp and Ripply proteins comprise a feedback loop wherein *Ripply2*, shown in mouse to be a direct target of Mesp2, is activated and in turn represses *mesp2* expression (Kawamura et al., 2005; Morimoto et al., 2007). Thus, as cells in the PSM progress through the segmentation

process, a variety of transcriptional inputs activate, refine and extinguish the expression of *Mesp* genes.

Mesp gene expression is also regulated in the PSM by a gradient of Retinoic Acid (RA) that is produced in the somitic mesoderm by RALDH2 and degraded in the tailbud by CYP26 (Moreno and Kintner, 2004). RA acts in the PSM in part by suppressing FGF signaling either by downregulating *FGF8* RNA as shown in the chick (Diez del Corral et al., 2003), or by inducing *MKP3*, a MAP kinase phosphatase in frog (Mason et al., 1996; Moreno and Kintner, 2004). By suppressing FGF8 signaling, RA shifts the differentiation wavefront posteriorly, leading to changes in segmental size. In addition, recent work in chick, mouse and zebrafish suggests that RA is an important factor that maintains bilateral symmetry during segmentation. In RA-depleted embryos, segmentation on the left side progresses more quickly than the right, presumably due to the effects of the left-right signaling machinery (Kawakami et al., 2005; Vermot et al., 2005; Vermot and Pourquie, 2005). This suggests that here, too, the role of RA is to influence the differentiation wavefront to maintain symmetry.

In *Xenopus* embryos, RA also directly activates the expression of *mespb* (previously referred to as *Thylacine1*, see Supp. Fig. 1) within the anterior PSM (Moreno and Kintner, 2004). By regulating the expression of *Mesp* genes directly, RA could conceivably influence either the boundary of *Mesp* expression, or its expression level along the A-P segmental axis. However, it is not clear whether a direct RA input into segmental gene expression is a conserved aspect of this patterning process. Here we examine these issues further, by analyzing RA regulation of the segmental patterning genes in fish and amphibians. Our results reveal a marked difference in the way these vertebrates respond to RA, and that this difference may be one way to modulate segmental patterning in a species-specific manner.

RESULTS

Genomic organization of the *Xenopus Mesp* genes

Genes encoding the Mesp proteins are found clustered in a tandem array in all of the vertebrate genomes sequenced thus far, including the mouse genome, where they are oriented head-to-head (Saga, 1998), and the zebrafish (Sawada et al., 2000) and pufferfish (Tr) genomes, where they are oriented head-to-tail (Fig. 1A). Recent completion of the *Xenopus tropicalis* genome also predicts two *Mesp* genes oriented head-to-head, with a third potential *Mesp* gene located in the intervening region. ESTs corresponding to third *Mesp* gene have not yet been reported. Mesp orthology is clear within mammalian and fish genomes, but between vertebrate lineages (e.g. fish *vs* mammal or amphibian *vs*. fish), the Mesp paralogs found within a species are more related to each other than to the putative orthologs in other species (Supp. Fig. 1), suggesting that they may have arisen either by duplication or through gene conversion events that occurred independently in each major vertebrate lineage. The apparently dynamic nature of the *Mesp* locus may contribute to variability in *Mesp* coding sequences and regulatory regions.

Xenopus contains a second segmentally expressed *Mesp* gene

Since only one of the *Mesp* genes has been characterized in any detail in *X. laevis* (Sparrow et al., 1998), we examined the expression pattern of the second gene, *mespa*. Since *Mesp* genes from different species will be examined in this study, we will designate the species of origin in the gene name (e.g. *Xl-mespa*) hereafter to avoid confusion. By whole-mount *in situ* hybridization, *Xl-mespa* expression was detected from early neurula through late tailbud stages, and was found exclusively in the PSM in a striped pattern (Fig. 1B) that resembled the expression of *Xl-mespb* (Fig. 1C). The PSM can be subdivided into three domains: a posterior 'tailbud' (TBD) region where unspecified cells reside, followed by a 'transition zone' (TZ) in which cells are specified to a segmental fate, and finally an anterior 'somitomere' domain, in which cells have acquired segmental pattern including A-P character within the future segments, but do not display morphological boundary formation (Fig. 1M). The onset of *Xl-mespb* expression is at the newest somitomere, or S-III, in frog embryos, and persists in older somitomeres, resulting in two to three stripes of expression in the PSM depending on the stage of the embryo (Fig. 1M). While similar, the expression of *Xl-mespa* appeared to be delayed by one somitomere relative to the onset in expression of *Xl-mespb* (Fig. 1B, C). Double *in situ* labeling confirmed this delay and showed that both genes mark the segmental boundary and overlap in the anterior half-segment (Fig. 1D). Thus, the expression of *Xl-mespa* is similar to *Xl-mespb* in maturing segments, but it is not expressed in S-III, the newest somitomere where segmental expression of *Xl-mespb* is established.

One hallmark of *Xl-mespb* expression in the transition zone is rapid, direct upregulation in response to RA treatment or when protein synthesis is blocked with cycloheximide (CHX) treatment (Moreno and Kintner, 2004). After treating embryos with RA for 1 hour, for example, the expression of *Xl-mespb* is strongly upregulated in S-III, as well as posterior to where the newest stripe of expression would normally form (Fig. 1H). As has been previously shown, a short treatment with CHX induces the expression of *Xl-mespb* in the transition zone (Kim et al., 2000; Moreno and Kintner, 2004), and also in the tailbud in a manner that synergizes with RA treatment, showing that *Xl-mespb* is likely a direct target of RA signaling (Fig. 1J, Moreno and Kintner, 2004). By contrast, the expression of *Xl-mespa* is either unchanged after a 1-hour treatment with RA or downregulated (Fig. 1G, data not shown). *Xl-mespa* is mildly de-repressed by treatments with CHX (Fig. 1I) but co-treatment of RA + CHX does not cause the strong response that is seen with *Xl-mespb* (Fig. 1K *vs* L). Thus, these results indicate that while the *Mesp* paralogs in *Xenopus* are both segmentally expressed, they vary in terms of how they respond to treatment with RA.

Fugu Mesp genomic sequences drive segmental expression in frogs

A 3.5 kb fragment lying upstream of the *Xl-mespb* is sufficient to recapitulate the segmental expression of endogenous *Xl-mespb* expression when introduced into transgenic embryos (Moreno and Kintner, 2004). This fragment is also upregulated by RA treatment through a response element that maps to a distal site. To determine whether a similar response element is present in the *Mesp* genes of other species, we examined *Mesp* orthologs in the pufferfish *Takifugu rubripes* (*Tr*) because of its highly compacted genome which would presumably allow control elements to be more easily mapped (Aparicio et al., 2002; Brenner et al.,

1993). Roughly 3 kb upstream of the fugu *Mesp* genes (*Tr-mespb* and *Tr-mespa)* coding sequences were cloned by PCR from genomic DNA. The fugu genes were compared with other vertebrate *Mesp* genes to ascertain their orthology (see Supplemental Fig. 1). Both genes were subsequently shuttled into the same *GFP* reporter vector as was used for the *Xl-mespb* gene, and introduced into *X. laevis* embryos using sperm transgenics. All transgenes contain a 3'UTR that confers instability to *GFP* RNA, a known feature of segmentally expressed genes (Davis et al., 2001; Moreno and Kintner, 2004).

Xenotransgenic embryos made with the *Tr-mespa* construct expressed *GFP* in the somitomere domain at fairly low levels, but this expression often lacked refined stripes so that it resembled a blur throughout the region (Fig. 2B). Furthermore, when the embryos were treated with RA, the pattern of *Tr-mespa* expression was unchanged. In contrast, the sequences upstream of *Tr-mespb* drove *GFP* expression in the PSM in a segmental pattern that closely resembled the pattern generated by the 3.5 kb *Xl-mespb* enhancer (compare Fig. 2A and 2C). While the *Tr-mespb* transgene on average produced stripes of expression that were broader than those of the endogenous *Xl-mespb* gene (data not shown), their expression domains were apparently in register at the anterior boundaries of half-segments when compared by two-label *in situ* hybridization (Fig. 2H, see 2I for schematic). The *Tr-mespb* transgene was also highly RA-responsive. After 1 hour of RA treatment, expression from the *Tr-mespb* transgene was strongly upregulated across the entire PSM from the somitomere region caudally to the tip of the tailbud (Fig. 2C). The *Tr-mespb* transgene also responded strongly to RA treatment (Fig. 2E) both in the presence and absence of CHX (Fig. 2E vs 2G), indicating that this response is likely to be direct as we observed with the *Xl-mespb* transgene (Fig. 2G and 1L; Moreno and Kintner, 2004). Thus, despite the evolutionary time separating these two species (Kumar and Hedges, 1998), the *Tr-mespb* upstream regulatory sequences retain the ability to drive a segmental, *Mesp*-like expression in the frog (Fig. 2I), and behave as a direct target of RA in the PSM.

RA and stripe response elements are distinct and organized similarly in fugu and *Xenopus* promoters

We next asked whether the inputs within the *Tr-mespb* transgene that drive RA response in the PSM are organized in a similar manner as those in *XMespβ.* When the *Xl-mespb* transgene was truncated from -3500 down to -1760 nucleotides (named *Xlmespb-Stu*, see Fig. 3A), the shorter version no longer responded to RA but was still expressed in stripes (compare Fig. 3B to C). A similar truncation of the *Tr-mespb* transgene from –2900 to -1545 [*Tr-mespb* (-1545)] also eliminated the response to RA while retaining stripe expression (Fig. 3E). Thus the *Tr-mespb* stripe enhancer is located promoter-proximally while its ability to respond to RA is dependent on a distal element upstream of position -1545.

The genomic sequences upstream of –1545 of *Tr-mespb* contain a retinoic acid response element (RARE) known as a βRE for its similarity to the RA response element in the *RARβ* gene, located between positions -1711 and -1694 (see Fig. 3A). To test whether this element is responsible for the RA responsiveness of *Tr-mespb*, we mutated each of the two half sites, in the context of the full-length *Tr-mespb* construct (*Tr-mespbmut*). Transgenic embryos expressing this point mutant construct drove *GFP* in somitomere stripes but failed to

respond when treated with RA, suggesting that the element responsible for RA induction was inactivated by the mutation (Fig. 3F). Together these results indicate that a distal element, involving a βRE, mediates the direct response of *Tr-mespb* to RA.

The regulation of *Mesp* genes by RA is complex

The results above show that a βRE element in the *Tr-mespb* enhancer is required for the *Tr-mespb* transgene to respond to RA. By contrast, an identifiable βRE element is not present in the *Xl-mespb* enhancer nor is there a region of the *Xl-mespb* enhancer upstream of the *Xl-mespb-Stu* fragment that shares obvious sequence homology with the *Tr-mespb* RA response region. These observations suggest that the RA response element in *Xl-mespb* could be a cryptic site, involve multiple divergent RA elements, or that it is more complex, involving not only RA elements but other cofactors as well. Since a functional βRE was identified in the fugu regulatory sequences, the sequences around the βRE were used as a starting point to define an RA response element that would be active during segmental patterning. To this end, we assayed the RA response of these sequences by fusing them onto the *Xl-mespb* stripe enhancer (*Xl-mespb-Stu*) and producing transgenic *X. laevis* embryos. Initially, a 250-bp region centered on the βRE in *Tr-mespb* was fused onto the 5' end of *Xl-mespb-Stu* (*Stu+P^{250}*; see Fig. 4A). This transgene showed full RA responsiveness (Figs. 4B-D), in that transgenic embryos treated with RA showed upregulation in stripes, broadening of stripes, and an anterior-to-posterior induction of tailbud expression. This response was dependent on the βRE, since point mutations in the half-sites abolished the upregulation in response to RA (*Stu+P^{250mut}*; Fig. 4E).

We next asked whether the RA response conferred by the 250-bp fragment was due solely to the βRE or was more complex. Chimeras creating by fusing the 17-bp *Trmespb* βRE sequence to *Xl-mespb-Stu* were as unresponsive to RA as *Xl-mespb-Stu* alone (*Stu+P^{17}*: compare Fig 4B to F). Similarly, RA did not induce a 30bp element containing the *Tr-mespb* βRE plus additional neighboring sequences (*Stu+P^{30}:* Compare Fig. 4B, to G) that was appended to *Xl-mespb-Stu*. A 95 bp fragment centered on the βRE (*Stu+P^{95}*) also did not respond to RA when appended to *Xl-mespb-Stu* (Fig. H). These results suggest that RA responsiveness may require cofactors that bind additional sites in the P^{250} fragment.

To determine whether this response was due to multiple RA inputs that may be cryptic in the *Tr-mespb* P^{250} fragment, we added two or four copies of a DR5 βRE (RA half-sites separated by 5 nucleotides (Rastinejad, 2001) to the *Xl-mespb-Stu* fragment (Fig. 4J, K). While we did see modest induction by RA of *GFP* in the tailbud of multiple-copy βRE embryos (*Stu+βRE^{2x}* and *Stu+βRE^{4x}*; Fig. 4J, K), this RA response differed both quantitatively and qualitatively from that of endogenous *Xl-mespb*, the full-length *Xl-mespb* transgene reporter (Fig. 4C), or the *Xl-mespb-StuP^{250}* fragment (Fig. 4D). All of these respond to RA first by intensifying and broadening the posterior somitomere expression domain, resulting in expression of *GFP* or of *Xl-mespb* through the entire tailbud in an anterior to posterior spread. By contrast, the two- and four-copy βRE insert constructs responded weakly to RA, and this response was not graded along the A-P axis, nor did it cause a change in stripe width. Thus, the additional retinoic acid response elements (RAREs) conferred a degree of RA responsiveness in the appropriate tissues, but could not

restore the RA response seen with *Xl-mespb* or the full-length transgene. Taken together, these results suggest that the response of *Tr-mespb* and *Xlmespb* to RA is not simply due to the presence of RA response elements. Instead, the simplest model is that other still-unknown PSM factors cooperate with RA, and the balance of these factors acting on the *Mesp* transgenes determines whether RA induction can occur.

Zebrafish *Mesp* genes are not induced by RA

The results with the Mesp genes in *X. laevis* and fugu indicate that within these species, one of the Mesp homologs (*Xl-mespb, Tr-mespb*) is strongly upregulated in response to RA while the other is not (*Xl-mespa, Tr-mespa*). To expand on these results, we asked whether the zebrafish (*D. renio) Mesp* genes, *Dr-mespa* or *Dr-mespb*, respond to RA in a similar manner. Strikingly, neither gene was induced, but instead both were markedly downregulated after longer periods of RA treatment (Fig. 5A, B, Supp. Fig. 3). Since in *X. laevis*, the induction of *Xl-mespb* by RA is synergistically enhanced by co-treatment with CHX (e.g. Fig1L), we also treated zebrafish embryos with both RA and CHX. CHX blocked the inhibitory effects of RA on *Dr-mespb* but did not reveal any masked upregulation in response to RA (Supp. Fig. 3). Thus, both *Mesp* homologs in Zebrafish do not appear to be activated by RA, but rather tend to be repressed. Moreover, the ability of RA to repress the expression of *Dr-mespb* depends on de novo protein synthesis, suggesting an indirect action.

XMespβ transgene is RA-responsive in zebrafish embryos

The different RA response of the *mesp* genes in *X. laevis* and zebrafish could be interpreted as a species difference in how the PSM responds to RA, or in the regulatory regions that drive *mesp* gene expression. To address the first possibility, we assessed how the PSM of zebrafish embryos responds to RA by examining the expression of *mespo*, a marker of undifferentiated PSM (Joseph and Cassetta, 1999) and *MKP3*, an inhibitor of the FGF signaling pathway (Keyse, 2000). RA downregulated *mespo* expression and upregulated *MKP3* expression in the Zebrafish PSM (Fig. 5C,D), indicating that RA treatment alters the differentiation wavefront in the zebrafish PSM as seen in *X. laevis* (Moreno and Kintner, 2004). To address the second possibility, we asked whether *Xl-mespb* enhancer driving *GFP* (*Xl-mespb-GFP*), when introduced into transgenic zebrafish, behaves the same way as it does in *X. laevis* or whether it takes on the pattern similar to a zebrafish *mesp* gene. A stable *Xl-mespb-GFP* transgenic line that was generated in zebrafish (see Materials and Methods) expressed GFP protein exclusively in somites, beginning at late epiboly and proceeding throughout somitogenesis stages (see Supplemental Fig. 2). By the 6-somite stage, two to three bands of expression were visible (Fig. 5E panel i) which increased in number, so that by the 12-somite stage, *Xl-mespb-GFP* zebrafish embryos typically exhibited three to four bands of *GFP* in the PSM (Fig. 5H, compare panels i and iii).

To determine how accurately the *Xl-mespb-GFP* transgene mirrors the expression of the zebrafish Mesp genes, we localized *GFP* RNA in relation to that of *mespa* or *mespb*. Within the somitomeres, the stripes of *GFP* RNA expression were in register with those of *mespa* or *mespb* (Fig. 5E). In double-label staining, transgenic *GFP* RNA expression overlapped with *Dr-mespb* RNA (Fig. 5F ii) and was excluded from the posterior half of each somitomere as shown by non-overlap with *myoD* (Fig. 5F iii). We used confocal microscopy to image GFP

expressed from the *Xl-mespb-GFP* transgene relative to the AP axis of newly formed somites, both in transgenic *X. laevis* embryos (Fig. 5G panel i) and in the zebrafish *Xl-mespb-GFP* line (Fig. 5G panel ii). In both cases, high GFP expression abutted the anterior edge of the newly formed somites, and was low in cells on the posterior side of the somite. Together these results indicate that the expression of *Xl-mespb-GFP* transgene at the segmental boundary is similar in *X.laevis* and zebrafish embryos.

However, the expression of the *Xl-mespb* transgene in zebrafish somitomeres differs from the zebrafish *Mesp* genes in two respects. The onset of *Xl-mespb-GFP* expression in the PSM can be detected earlier than that of *Dr-mespa* or *Dr-mespb* (Fig. 5Ei, S-2), and in some cases was detectable in the tailbud (Fig. 5Ei, arrow), although this was variable (Fig. 5H i and iii). In addition, half-segmental expression of *Xl-mespb-GFP* tends to be broader than for the zebrafish *Mesp* genes (Fig. 5E i *vs* ii and iii). Both of these differences could be explained if the *Xl-mespb-GFP* transgene responds directly to RA even though the zebrafish *Mesp* genes do not. To test this idea, we treated the *Xlmespb-GFP* zebrafish with RA and stained for *GFP* RNA (Fig. 5H). While *Dr-mespa* RNA expression was downregulated by RA as shown above (Fig. 5A and Supp. Fig. 3), the expression of *GFP* within the PSM was markedly upregulated, independent of the developmental stage when treatment occurred (Fig. 5H i *vs* ii; iii *vs* iv), and this response was rapid (Supp. Fig. 3). Indeed the RA response of the *Xl-mespb-GFP* transgene in fish mirrored the RA response of *Xl-mespb* in *X. laevis* embryos: broader stripes, stronger expression in the stripes, and early activation in the forming stripe in the PSM (Fig. 5H). Together, these results indicate that the *Xl-mespb-GFP* transgene can respond to RA in zebrafish, suggesting that factors required for this response are still present in the cellular context of the zebrafish PSM, and are capable of acting on the frog genomic regulatory sequences. Notably, while this direct response changes A-P segmental expression, it apparently does not change expression at the segmental boundary.

The converse experiment is to assay the segmental expression of *Dr-mespa* and *Dr-mespb* in *X. leavis* transgenics. However, when we isolated and tested a 8.4kb and 3.2kb upstream region from *Dr-mespa* or *Dr-mespb*, respectively, neither was able to drive detectable expression in the PSM of transgenic *X. laevis* embryos (data not shown). Nonetheless, we note that the *Xl-mespb* and *Tr-mespb* transgenes lacking the RA response region tend to drive expression in *X. laevis* in a pattern similar to that observed for *Dr-mespa* and *Dr-mespb*. For example, when the RA response element is absent from the *Xl-mespb* and *Tr-mespb* transgenes, the frequency of transgenesis markedly drops upon RA treatment (data not shown and Supp. Fig.3). Therefore, removing a direct RA response from the *Xl-mespb* segmental enhancer seems to switch the RA response from upregulation to downregulation as observed with the Zebrafish *Mesp* genes.

Ripply genes modulate the RA response in the PSM

The results above show that some *Mesp* paralogs are strongly induced by RA as direct targets, while others are downregulated following longer treatment periods (see Fig. 1 for frog, Fig. 5 for zebrafish). The latter observation suggests that RA might influence the expression of repressors that inhibit *Mesp* expression during segmental patterning. We therefore examined the Ripply family of co-repressors, which are known to function in a

negative feedback loop with the Mesp proteins to ensure that *Mesp* gene expression is rapidly extinguished prior to somitogenesis (Chan et al., 2006; Kawamura et al., 2005; Kondow et al., 2006; Morimoto et al., 2007). Specifically, we asked whether RA downregulates the expression of the *Mesp* genes in zebrafish via changes in the expression of the *Ripply* genes.

We surveyed the *Ripply* genes in *X. laevis* and zebrafish for RA responsiveness and observed that several were induced by RA treatment. In zebrafish embryos, *ripply1* expression was induced throughout the tailbud domain while *ripply2* expression was induced caudal to its posterior stripe of expression (Fig. 6A). RA induced the expression of both genes in the presence of CHX, suggesting a potentially direct action. In *X. laevis* embryos treated with RA, a ripply-like gene, *Bowline* (Kondow et al., 2006), was induced in the PSM in a pattern indistinguishable from the response of *Xl-mespb* (Fig. 6B). RA induction of *bowline* also occurred in the presence of CHX, suggesting a direct affect. A second *X. laevis Ripply* gene, *ledgerline*, is expressed segmentally (Chan et al., 2006) but did not respond to RA or RA + CHX (Fig. 6B) while a third *X. laevis Ripply* gene (NIBB clone XL018m04) was expressed in heart mesoderm but not in paraxial mesoderm (data not shown). Therefore, both *X. laevis* and zebrafish have at least one member of the Ripply family that can be induced in the PSM by RA, perhaps directly.

We next inhibited Ripply function in zebrafish embryos by injecting morpholino that targeted *Ripply1* (*Ripply1*^{mo}) or *Ripply2* (*Ripply2*^{mo}). As reported previously, injecting *Ripply1*^{mo} into zebrafish embryos produces a marked upregulation of *Dr-mespa* and *Drmespb* expression within somites (Kawamura et al., 2005). Neither *Mesp* gene was changed in Zebrafish embryos injected with *Ripply2*^{mo} alone, but when embryos were injected with both morpholinos, the expression of both *Mesp* genes were dramatically upregulated in the PSM, resulting in a loss of stripe expression (Fig. 6C and D). This result suggests that the Ripply proteins are not only used to extinguish the expression of the *Mesp* genes prior to somitogenesis (Kawamura et al., 2005), but also to confine their expression to the anterior half-segment during segmental patterning. Moreover, in embryos injected with the anti-*Ripply* morpholinos, the downregulation of the *Mesp* genes by RA was blocked (Fig. 6C and D). Thus, RA induction of the *Ripply* genes may be one factor causing the downregulation of the *Mesp* genes.

If *Xl-mespb* expression were insensitive to Ripply repression, this would help explain why it fails to be downregulated after treatment with RA. To address this possibility, we first asked whether the zebrafish *Xl-mespb-GFP* embryos injected with *Ripply1* morpholinos exhibited the same type of upregulation as the zebrafish *Mesp* genes. Indeed, *GFP* expression was markedly upregulated (Fig. 6E) in a similar manner to the endogenous *Mesp* genes, suggesting that the *X.laevis* enhancer is also responsive to Ripply-mediated repression. Similarly, endogenous expression of *Xl-mespb* was inhibited in *Xenopus* embryos that overexpress *X. laevis ledgerline* and/or *bowline* by RNA injection. Notably, overexpressing either *Ripply* family member also blocked the RA induction of *Xl-mespb* expression (Fig. 6F-I). Together, these results indicate that Ripply proteins repress *Xl-mespb* both in the transgenic fish and within *Xenopus* embryos. Our results further suggest that the inhibitory effects of Ripplys on *Mesp* expression can be modulated by the presence of a direct RA

response element, such that *Mesp* is upregulated even when RA concurrently induces Ripply-like factors.

DISCUSSION

Here we use a cross-species analysis to examine the mechanisms that regulate the segmental expression of the Mesp family of bHLH transcription factors. On one hand, our results show that a promoter fragment taken from one species and introduced into another is expressed to a large degree in the proper segmental pattern for the host, indicating that many of the transcriptional inputs that drive the segmental expression of the *Mesp* genes are conserved. On the other, we show that the regulation of Mesp homologs can show species-specific differences and that one significant difference is the ability to directly respond to transcriptional activation by RA. This RA response occurs in balance with their repression by the Ripply co-repressors, which we show also to be RA targets. Our results indicate that this balance does not appear to change the boundary of segmental expression, but rather the level of *Mesp* expression within a segmental unit along it A-P axis. We speculate that species differences in how RA influences the Mesp-Ripply feedback loop during segmentation may underlie variation between species in A-P segmental patterning.

Genomic organization of Mesp genes

Two neighboring *Mesp* paralogs are found in the genomes of all vertebrates sequenced thus far (Saga, 1998; Sawada et al., 2000; Terasaki et al., 2006). Based on homologies of the proteins they encode, the two genes appear to have arisen by either an independent duplication or have been modified by gene conversion within each major vertebrate lineage. As a consequence, the two *Mesp* genes presumably have undergone significant variation across species in terms of both their coding sequences and the regulatory elements that control their expression patterns, resulting in different patterns for *Mesp* pairs in certain species. In mouse, for example, *Mesp1* is expressed segmentally but also in early mesoderm and heart, while in *X. laevis*, the *Mesp* paralogs are both expressed in somitomeres but neither is detectable outside of the PSM during developmental stages.

The dynamic nature of this locus provides an opportunity for variation to arise in the expression patterns of the two *Mesp* paralogs in ways that lead to difference in segmental patterning. Marked differences exist in the way that each paralog is expressed during segmental patterning. In *X. laevis* embryos, for example, *Xl-mespa* is expressed one segmental unit later than *Xl-mespb* and does not respond directly to RA, but shares the same anterior boundary of expression within a segment as *Xl-mespb.* Thus, the regulatory elements that drive the *Mesp* expression in the PSM have undergone significant variation both within and between species. To examine the consequences of these variations, we used a xenotransgenic approach to compare regulatory elements.

The Fugu *Mespb* promoter is expressed segmentally in *Xenopus* embryos and is RA responsive

When the *Tr-mespb* promoter region is introduced into *X. laevis* embryos, its expression pattern in the PSM is remarkably similar to that of the *Xl-mespb* gene. This result is

compelling evidence that the *Tr-mespb* gene responds to segmental patterning cues in *Xenopus* embryos in an appropriate fashion for a segmentally expressed gene, even though these two species are separated by millions of years of evolutionary time. Like the *Xl-mespb* promoter fragment, the fugu gene also responds strongly to treatment with RA and this response is mediated through an element we localized to the upstream half of the cloned sequences. Indeed, the fugu response to RA appears on average more robust than the response observed with the *Xl-mespb* enhancer in transgenics or with the endogenous gene, an observation that could be due to the fact that the fugu promoter contains a bonafide RARE element, which is required for fugu RA responsiveness in transgenic frogs, based on our analysis of a point mutant. By contrast, even though the *Xl-mespb* gene appears to respond directly to RA, analysis of the promoter sequences does not reveal a conserved RARE element, or a region with significant homology to the fugu region that responds to RA.

To address this paradox, we further characterized the RA response element in the fugu regulatory sequences, by generating and testing compound enhancers where the fugu RA response element was appended to the *X. laevis* stripe enhancer. This analysis indicates a 250 bp fragment of fugu sequence centered around the bRE were required to initiate a full RA response in the compound enhancer in a pattern that closely resembles the RA response of the *Xl-mespb* gene, either endogenous or transgenic. By contrast, in simple constructs where two or four added bREs were used in a compound enhancer, the transgene was able to respond to RA by general upregulation in the PSM and somitomere tissue, but this did not follow the endogenous pattern either quantitatively or qualitatively. Our interpretation of these results is that the RA response element is likely to be complex, involving a binding site for the RA receptor that works cooperatively with binding sites for other factors that are present in the PSM. These observations emphasize the difficulty of identifying response elements for factors that act in a highly specific tissue context. Clearly, using simple multimerized binding sites to infer where a factor such as RA is transcriptionally active in a developing tissue is insufficient to reveal the whole picture of its activity in that tissue.

The *Xenopus Mespβ* gene is expressed segmentally in zebrafish embryos and is responsive to RA

RA treatment of zebrafish embryos inhibits the expression of both *Dr-mespa* and *Dr-mespb* while in *X. laevis* the opposite result is obtained with *Xl-mespb* or the *Tr-mespb* transgene. This differential response could be due to the way that the PSM in different species responds to RA, or to differences in how the *Mesp* genes are organized in different species. Several observations support the latter over the former possibility. First, RA treatment of zebrafish embryos affects the tailbud marker *mespo* and the ERK inhibitor *MKP3* in a similar way as reported in *Xenopus* (Mason et al., 1996; Moreno and Kintner, 2004). Second, the RARE element found upstream of *Tr-Mespb* gene does not appeared to be conserved in the zebrafish *Mesp* genes by sequence alignment (data not shown). Third, when the *Xl-mespb* enhancer is introduced into zebrafish embryos as a transgene, it retains the ability to directly respond to RA. Indeed, this direct response can account for subtle differences that occur when comparing the expression of the *Xlmespb-GFP* transgene to that of the zebrafish *Mesp* genes. The *Xl-mespb-GFP* transgene, for example, tends to be expressed with an earlier

onset, in that its expression is first apparent in the PSM during the transition between the caudal, undifferentiated PSM and the somitomere domain. By comparison, the zebrafish *Mesp* genes are activated at a slightly later point. Moreover, the *Xl-mespb-GFP* transgenic expression within the segment appears to be broader than either endogenous zebrafish *Mesp* gene. While we cannot rule out that these differences are due to other factors such as transgene copy number, they are consistent with the idea that the direct RA response element allows the *X. laevis* transgene to respond to RA in the transition zone, resulting in an earlier onset and more robust expression in the anterior half segment.

By comparing the expression of the *Xl-mespb-GFP* transgene to that of the zebrafish *Mesp* genes, we can assess how the loss of a direct RA response element might contribute to the segmental expression of these genes. Importantly, in zebrafish, the expression of the *Xl-mespb-GFP* transgene abuts the same segmental boundary as the zebrafish *Mesp* genes. The implication of this result is that the presence or absence of a direct RA response element is not likely to shift the anterior limit of *Mesp* expression relative to a segmental boundary. Instead, our results indicate that the direct RA response mostly likely alters the levels of *Mesp* gene expression within the segment itself, perhaps altering the proportion of cells assigned to the anterior and posterior fates.

Ripply genes modulate the effects of RA during segmentation

While the lack of an RA response element in the zebrafish gene explains why these genes are not upregulated in response to RA, it does not explain why they are downregulated. We therefore examined whether this repression involves the *Ripply* proteins, which are known to act as negative feedback regulators of the *Mesp* genes. We found that in both zebrafish and *X. laevis* embryos, RA induces the expression of *Ripply* genes in the PSM. Moreover in zebrafish, the ability of RA to repress the *Mesp* genes is abolished by reducing the activity of the *Ripply* genes using morpholinos. *Ripplys* are therefore one factor that determines the response of the *Mesp* genes to RA treatment.

RA also induces the expression of *Bowline*, a *Ripply* factor in *X. laevis*. Moreover, in gain-of-function experiments, expression of *Xl-mespb* is strongly repressed by *Bowline* even in the presence of RA. Furthermore, expression of *Xl-mespb-GFP* in transgenic zebrafish is also notably upregulated when ripply function is impaired. These observations suggest strongly that the *Xl-mespb* enhancer has a Ripply-mediated repressive input that is likely to be induced further by RA. However, we suggest that the *Xl-mespb* enhancer has the ability to overcome this repressive input based on the presence of a direct RA response element. In this model, the lack of an RA response element in the *Mesp* genes in zebrafish shifts the balance of RA input toward *Ripply* induction and thus toward *Mesp* repression. Consistent with the model, a similar shift is seen in transgenic experiments when the RA response element is deleted from the *Xlmespb-GFP* transgene. For example, when *Xl-mespb-Stu* transgenics were treated with RA, a significant fraction of these embryos lost expression of the transgene when compared to mock-treated *Xl-mespb-GFP* sibling controls (Supp. Fig. 3). In other words, removing the RA response element from *Xl-mespb-GFP* shifts the balance so that RA treatment results in the opposite response, downregulation.

Evolution of segmentation mechanisms

In light of these results, we propose a model to explain how the *Mesp* paralogs in different species respond to RA based on the presence or absence of a direct RA response element. This model is based on the idea that RA has multiple input points in the feedback loop between *Mesp* and *Ripply* genes, with certain species favoring RA input on the *Ripply* side (zebrafish) while others favor input on the *Mesp* side (frog and perhaps fugu). In the former case, *Mesp* gene expression is likely to be repressed more effectively by the *Ripply* genes during segmental patterning, resulting in a shift of expression towards the anterior side of the segment. In the latter, the presence of the RA element promotes expression of the *Mesp* genes, shifting the width of segmental expression posteriorly. These shifts are clearly seen in the difference between the expression limits in the zebrafish PSM of the *Xl-mespb*-transgene that contains an RA response element and the zebrafish *Mesp* genes that do not. As a consequence, we speculate that changing how the *Mesp* genes respond to RA may be a way to shift the assignment of somitic cells to anterior and posterior fates. For example, the anterior cells in zebrafish segments rotate to the outside of the somite, where they contribute to distinct fates, including muscle progenitors, and hypaxial muscles (Hollway et al., 2007). One can imagine that changes in the size of this anterior population could vary in different species, and this could be driven by changes in the RA response. The best direct test of this model in the future is to eliminate or add RA responsiveness to *Mesp* genes in different species and determine whether this has the predicted effects on A-P patterning and the fate of somitic derivatives.

Materials and Methods

Xenopus laevis fertilizations, microinjections and embryo culture

X. laevis embryos were obtained by *in vitro* fertilization of pigmented and albino animals, according to established methods (Sive et al., 2000). Embryos were staged according to the normal tables of Nieuwkoop and Faber (Nieuwkoop and Faber, 1967).

Capped messenger mRNA was generated *in vitro* using SP6 RNA polymerase from DNA templates based on the CS2 vector (Turner and Weintraub, 1994). Embryos were injected into the marginal zone of one cell at the two-cell stage for whole embryo experiments. Embryos were cultured until the indicated stage in 0.1 X MMR (Sive et al., 2000) plus Gentamycin, then fixed for 1 hour in MEMFA (Sive et al., 2000), and stored in 100% ethanol until further processing. All injection experiments were performed at least twice; results shown are representative. Doses: embryos injected with 1ng for ledgerline, or 200pg for *bowline* were severely dorsalized and many exhibited double axes including head tissue. Lower dose injections (400pg ledgerline, 80pg *bowline*) resulted in embryos with normal overall morphology but which had varying degrees of loss of *Mesp* gene expression on the injected side, in accordance with published results in frog and fish (Chan et al., 2006; Kawamura et al., 2005; Kondow et al., 2006)}. *nlacZ* RNA was used as a lineage tracer at 100pg or as an injection control at the same dose as was used in experimentals.

For zebrafish morpholino experiments: embryos were injected at the 1-4 cell stages into the yolk with: R1 MO (anti-*Ripply1*, GeneTools LLC) was as previously published by

Kawamura et al (2005), R2 MO (anti-*Ripply2*, GeneTools LLC): 5′-TCGTGAAAGTGATGTTCTC**CAT**AGT-3′ (start codon is in bold print), or both. Morpholinos were resuspended at 1mM and injected at dilutions of 1:5 and 1:10 in Daneiau's solution with Phenyl Red as a tracer. Embryos were cultured in Embryo Medium (EM) (Westerfield, 2000) until stages of interest when they were treated with drug (see below) or fixed in 4% paraformaldehyde in PBS for further processing. Embryos were dechorionated after drug treatments when treated with RA.

Identification and isolation of *Xl-mespa*

The sequence of the *X. tropicalis* genome identifies two *Mesp* genes as found in other vertebrate species. These two genes are denoted as *mespa* and *mespb* without inferring syngeny with the *Mesp* genes in other species (Suppl. Fig. 1). Based on this nomenclature, the *Thylacine* gene in *X. laevis* is now referred to *mespb* while the ESTs in the *X. laevis* database that correspond to *X. tropicalis mespa* are referred to *mespa*. Plasmids encoding *Xl-mespa* (XL194g13 and XL218m17) were kindly provided by the NIBB consortium (Japan). Both were tested by *in situ* hybridization and were found to have identical expression patterns.

Subcloning of the *XMespβ* regulatory sequences and transgenic methods

Cloning of the *Xl-mespb* regulatory sequences from genomic DNA was reported in Moreno and Kintner, 2004. Deletion constructs were generated using unique restriction sites within the promoter sequences. *X. laevis* transgenics were generated using the protocol of Kroll and Amaya (Kroll and Amaya, 1996) with modifications described by Sparrow et al. (Sparrow et al., 2000).

Sequences upstream of Tr-*mespa* and *b* were cloned from genomic DNA using the following primers: for *Tr-mespb*:

downstream: 5′-TAAAGGATCCAATGTGAGGAGAGACTTGCT-3′,

upstream; 5′-TATTGTCGACTGCAAAGGTCAACCTCTTAC-3′;

For *Tr-mespa*:

downstream: 5′- GCAAAGATCTAGCTACTGTTGCAGTCGTAGTC-3′,

upstream: 5′- TTTAGTCGACACACGCCAACACCTCTGC-3′.

These were inserted in the same transgenic vector including the 3′ UTR instability sequence as *Xl-mespb-GFP*. Constructs joining *Xl-mespb-Stu* with versions of the fugu RARE sequence were generated by PCR amplification of the sequence of interest followed by insertion at SalI - StuI of the *Xl-mespb-GFP* construct. Sequences are designated in the text. The P17 and P30 insertions were generated by annealing complementary oligo sequences with SalI-StuI ends and ligating into the SalI - StuI sequence of *XMespβ-GFP*. Fugu deletion contructs were generated using endogenous restriction sites. Point mutations in the fugu RARE was generated by site directed mutagenesis using the Stratagene Quik Change kit and oligos of the sequence:

top oligo: 5′CCAGTGTGGGT**AA**AGCCCCAGT**AA**AGTGTGCCCCC-3’,

bottom oligo: 5′- GGGGGCACACT**TT**ACTGGGGCT**TT**ACCCACACTGG-3′.

RA element half-sites are underlined; points mutated are in bold. *Stu-βRE*^{2x} and *Stu-βRE*^{4x} were synthesized by inserting the Klenow-blunted HindIII-SphI fragment from a TK-luc-twinDR5 plasmid (kind gift of Estelita Ong), which contains two RARE sites, into the StuI site of *Xl-mespb-GFP*. We chose one clone with a single insertion (*Stu-βRE*^{2x}) and a separate clone with a tandem insertion of two fragments (*Stu-βRE*^{4x}), both oriented in the same direction. The inserted twinDR5 sequence is:

5′**AAGCTT**AAAGGTCACCGAAAGGTCACCATCCCGGGAAAAGGTCACCGAAAGGTCACCAGCTT**GCATGC**-3′,

with RA half-sites underlined and HindII and SphI sites in bold.

The zebrafish *Xl-mespb-GFP* line was generated by injection of 100pg of NotI-linearized *Xl-mespb-GFP* DNA into 1-cell AB embryos. Resultant embryos were screened for GFP fluorescence in the somites and grown to maturity when they were bred inter se. Two embryos with somite GFP expression were grown to maturity and one was the founder of the line used in these experiments. Embryos used for drug treatments were hemizygous, generated by crossing either *Xl-mespb-GFP* +/+ zebrafish with wild-type AB, or by crossing hemizygous (+/−)*Xl-mespb-GFP* zebrafish with wild-type ABs.

In situ hybridization

Whole-mount *in situ* hybridization for frog and zebrafish embryos and explants was performed as described in (Harland, 1991) except that the acetic anhydride and RNAse steps were omitted, and in zebrafish *in situs*, the zebrafish recipe for hybridization buffer from (Westerfield, 2000) was used. Double *in situ*s were performed with digoxigenin- and fluorescein-labelled probes. Substrates for color detection were NBT/BCIP (Roche) and Fast Red (Roche). Pigmented *Xenopus* embryos were bleached after *in situ* hybridization (Sive et al., 2000). Probes for zebrafish *mespa*, *mespb*, *mespo*, and *ripply1*, *2*, and *3* were cloned by RT-PCR from 10-somite stage embryos using primers designed against published sequences.

Drug treatments

All-trans retinoic acid (Calbiochem) was used at 1μM; cycloheximide (Sigma) at 10μg/ml. RA was dissolved in DMSO, CHX in 100% ethanol and then diluted into 0.1 X MMR (frog experiments) or EM (zebrafish experiments). Carrier controls (DMSO alone or DMSO + ethanol) were performed at the highest solvent concentration that the experimental embryos received in each set. All drug-treatment experiments were performed at least three times independently. In each experiment, 10-12 embryos were examined per condition per probe, with a majority (>70%) exhibiting the phenotype shown. Numbers given in figures and legends are for one experiment.

Supplementary Material

Refer to Web version on PubMed Central for supplementary material.

Acknowledgements

The authors wish to thank members of the Belmonte laboratory for help, reagents, and advice on zebrafish work, especially C. Callol-Massot, I. Dubova, Y. Kawakami, C. Koth and A. Rojas. We thank Brian Mitchell, Alivia Price, and Jennifer Stubbs for critical comments on the manuscript, Gerard Manning for bioinformatics advice and Sydney Brenner for discussions. We are grateful to E. Ong for providing plasmids and Y. Mikawa for providing fugu genomic DNA. We are also grateful to Naoto Ueno and the NIBB *Xenopus laevis* EST project for generously providing clones. Work reported here was supported by NIH grants to CK and JCIB.

References

Aparicio S, Chapman J, Stupka E, Putnam N, Chia JM, Dehal P, Christoffels A, Rash S, Hoon S, Smit A, Gelpke MD, Roach J, Oh T, Ho IY, Wong M, Detter C, Verhoef F, Predki P, Tay A, Lucas S, Richardson P, Smith SF, Clark MS, Edwards YJ, Doggett N, Zharkikh A, Tavtigian SV, Pruss D, Barnstead M, Evans C, Baden H, Powell J, Glusman G, Rowen L, Hood L, Tan YH, Elgar G, Hawkins T, Venkatesh B, Rokhsar D, Brenner S. Whole-genome shotgun assembly and analysis of the genome of Fugu rubripes. Science. 2002; 297:1301–10. [PubMed: 12142439]

Aulehla A, Herrmann BG. Segmentation in vertebrates: clock and gradient finally joined. Genes Dev. 2004; 18:2060–7. [PubMed: 15342488]

Brand-Saberi B, Christ B. Evolution and development of distinct cell lineages derived from somites. Curr Top Dev Biol. 2000; 48:1–42. [PubMed: 10635456]

Brenner S, Elgar G, Sandford R, Macrae A, Venkatesh B, Aparicio S. Characterization of the pufferfish (Fugu) genome as a compact model vertebrate genome. Nature. 1993; 366:265–8. [PubMed: 8232585]

Buchberger A, Bonneick S, Klein C, Arnold HH. Dynamic expression of chicken cMeso2 in segmental plate and somites. Dev Dyn. 2002; 223:108–18. [PubMed: 11803574]

Buchberger A, Seidl K, Klein C, Eberhardt H, Arnold HH. cMeso-1, a novel bHLH transcription factor, is involved in somite formation in chicken embryos. Dev Biol. 1998; 199:201–15. [PubMed: 9698440]

Chan T, Satow R, Kitagawa H, Kato S, Asashima M. Ledgerline, a novel [i]Xenopus[/i] laevis gene, regulates differentiation of presomitic mesoderm during somitogenesis. Zoolog Sci. 2006; 23:689–97. [PubMed: 16971787]

Christ B, Huang R, Wilting J. The development of the avian vertebral column. Anat Embryol (Berl). 2000; 202:179–94. [PubMed: 10994991]

Christen B, Slack JM. FGF-8 is associated with anteroposterior patterning and limb regeneration in [i]Xenopus[/i]. Dev Biol. 1997; 192:455–66. [PubMed: 9441681]

Cooke J, Zeeman EC. A clock and wavefront model for control of the number of repeated structures during animal morphogenesis. J Theor Biol. 1976; 58:455–76. [PubMed: 940335]

Davis RL, Turner D, Evans LM, Kirschner MW. Molecular targets of vertebrate segmentation: two mechanisms control segmental expression of [i]Xenopus[/i] hairy2 during somite formation. Dev Cell. 2001; 1:553–565. [PubMed: 11703945]

Diez del Corral R, Olivera-Martinez I, Goriely A, Gale E, Maden M, Storey K. Opposing FGF and retinoid pathways control ventral neural pattern, neuronal differentiation, and segmentation during body axis extension. Neuron. 2003; 40:65–79. [PubMed: 14527434]

Dubrulle J, McGrew MJ, Pourquie O. FGF signaling controls somite boundary position and regulates segmentation clock control of spatiotemporal Hox gene activation. Cell. 2001; 106:219–32. [PubMed: 11511349]

Dubrulle J, Pourquie O. From head to tail: links between the segmentation clock and antero-posterior patterning of the embryo. Curr Opin Genet Dev. 2002; 12:519–23. [PubMed: 12200156]

Dubrulle J, Pourquie O. fgf8 mRNA decay establishes a gradient that couples axial elongation to patterning in the vertebrate embryo. Nature. 2004; 427:419–22. [PubMed: 14749824]

Gridley T. The long and short of it: somite formation in mice. Dev Dyn. 2006; 235:2330–6. [PubMed: 16724326]

Harland RM. [i]In situ[/i] hybridization: an improved whole-mount method for [i]Xenopus[/i] embryos. Methods Cell Biol. 1991; 36:685–95. [PubMed: 1811161]

Hollemann T, Chen Y, Grunz H, Pieler T. Regionalized metabolic activity establishes boundaries of retinoic acid signalling. Embo J. 1998; 17:7361–72. [PubMed: 9857192]

Hollway GE, Bryson-Richardson RJ, Berger Sl, Cole HJ, Halle TE, Currie PD. Whole-somite rotation generates msucle progenitor cell compartments in the developing zebrafish embryo. Dev. Cell. 2007; 12:207–219. [PubMed: 17276339]

Hrabe de Angelis M, McIntyre J 2nd, Gossler A. Maintenance of somite borders in mice requires the Delta homologue DII1. Nature. 1997; 386:717–21. [PubMed: 9109488]

Jen WC, Gawantka V, Pollet N, Niehrs C, Kintner C. Periodic repression of Notch pathway genes governs the segmentation of [i]Xenopus[/i] embryos. Genes Dev. 1999; 13:1486–99. [PubMed: 10364164]

Jen WC, Wettstein D, Turner D, Chitnis A, Kintner C. The Notch ligand, X-Delta-2, mediates segmentation of the paraxial mesoderm in [i]Xenopus[/i] embryos. Development. 1997; 124:1169–78. [PubMed: 9102304]

Joseph EM, Cassetta LA. Mespo: a novel basic helix-loop-helix gene expressed in the presomitic mesoderm and posterior tailbud of [i]Xenopus[/i] embryos. Mech Dev. 1999; 82:191–4. [PubMed: 10354484]

Kawakami Y, Raya A, Raya RM, Rodriguez-Esteban C, Belmonte JC. Retinoic acid signalling links left-right asymmetric patterning and bilaterally symmetric somitogenesis in the zebrafish embryo. Nature. 2005; 435:165–71. [PubMed: 15889082]

Kawamura A, Koshida S, Hijikata H, Ohbayashi A, Kondoh H, Takada S. Groucho-associated transcriptional repressor ripply1 is required for proper transition from the presomitic mesoderm to somites. Dev Cell. 2005; 9:735–44. [PubMed: 16326386]

Keyse SM. Protein phosphatases and the regulation of mitogen-activated protein kinase signalling. Curr Opin Cell Biol. 2000; 12:186–92. [PubMed: 10712927]

Kim SH, Jen WC, De Robertis EM, Kintner C. The protocadherin PAPC establishes segmental boundaries during somitogenesis in [i]Xenopus[/i] embryos. Curr Biol. 2000; 10:821–30. [PubMed: 10899001]

Kondow A, Hitachi K, Ikegame T, Asashima M. Bowline, a novel protein localized to the presomitic mesoderm, interacts with Groucho/TLE in [i]Xenopus[/i]. Int J Dev Biol. 2006; 50:473–9. [PubMed: 16586348]

Kroll KL, Amaya E. Transgenic [i]Xenopus[/i] embryos from sperm nuclear transplantations reveal FGF signaling requirements during gastrulation. Development. 1996; 122:3173–83. [PubMed: 8898230]

Kumar S, Hedges SB. A molecular timescale for vertebrate evolution. Nature. 1998; 392:917–20. [PubMed: 9582070]

Li Y, Fenger U, Niehrs C, Pollet N. Cyclic expression of esr9 gene in [i]Xenopus[/i] presomitic mesoderm. Differentiation. 2003; 71:83–9. [PubMed: 12558606]

Mason C, Lake M, Nebreda A, Old R. A novel MAP kinase phosphatase is localised in the branchial arch region and tail tip of [i]Xenopus[/i] embryos and is inducible by retinoic acid. Mech Dev. 1996; 55:133–44. [PubMed: 8861094]

Moreno TA, Kintner C. Regulation of segmental patterning by retinoic acid signaling during [i]Xenopus[/i] somitogenesis. Dev Cell. 2004; 6:205–18. [PubMed: 14960275]

Morimoto M, Kiso M, Sasaki N, Saga Y. Cooperative Mesp activity is required for normal somitogenesis along the anterior-posterior axis. Dev Biol. 2006; 300:687–98. [PubMed: 16996494]

Morimoto M, Sasaki N, Oginuma M, Kiso M, Igarashi K, Aizaki K, Kanno J, Saga Y. The negative regulation of Mesp2 by mouse Ripply2 is required to establish the rostro-caudal patterning within a somite. Development. 2007; 134:1561–9. [PubMed: 17360776]

Morimoto M, Takahashi Y, Endo M, Saga Y. The Mesp2 transcription factor establishes segmental borders by suppressing Notch activity. Nature. 2005; 435:354–9. [PubMed: 15902259]

Nakajima Y, Morimoto M, Takahashi Y, Koseki H, Saga Y. Identification of Epha4 enhancer required for segmental expression and the regulation by Mesp2. Development. 2006; 133:2517–25. [PubMed: 16728472]

Nieuwkoop, PD.; Faber, J. Normal table of [i]Xenopus[/i] Laevis. North Holland, Amersterdam: 1967.

Nomura-Kitabayashi A, Takahashi Y, Kitajima S, Inoue T, Takeda H, Saga Y. Hypomorphic Mesp allele distinguishes establishment of rostrocaudal polarity and segment border formation in somitogenesis. Development. 2002; 129:2473–81. [PubMed: 11973278]

Pourquie O. The vertebrate segmentation clock. J Anat. 2001; 199:169–75. [PubMed: 11523819]

Rastinejad F. Retinoid X receptor and its partners in the nuclear receptor family. Curr Opin Struct Biol. 2001; 11:33–8. [PubMed: 11179889]

Saga Y. Genetic rescue of segmentation defect in MesP2-deficient mice by MesP1 gene replacement. Mech Dev. 1998; 75:53–66. [PubMed: 9739106]

Saga Y, Hata N, Kobayashi S, Magnuson T, Seldin MF, Taketo MM. MesP1: a novel basic helix-loop-helix protein expressed in the nascent mesodermal cells during mouse gastrulation. Development. 1996; 122:2769–78. [PubMed: 8787751]

Saga Y, Hata N, Koseki H, Taketo MM. Mesp2: a novel mouse gene expressed in the presegmented mesoderm and essential for segmentation initiation. Genes Dev. 1997; 11:1827–39. [PubMed: 9242490]

Saga Y, Takeda H. The making of the somite: molecular events in vertebrate segmentation. Nat Rev Genet. 2001; 2:835–45. [PubMed: 11715039]

Sawada A, Fritz A, Jiang YJ, Yamamoto A, Yamasu K, Kuroiwa A, Saga Y, Takeda H. Zebrafish Mesp family genes, mesp-a and mesp-b are segmentally expressed in the presomitic mesoderm, and Mesp-b confers the anterior identity to the developing somites. Development. 2000; 127:1691–702. [PubMed: 10725245]

Sawada A, Shinya M, Jiang YJ, Kawakami A, Kuroiwa A, Takeda H. Fgf/MAPK signalling is a crucial positional cue in somite boundary formation. Development. 2001; 128:4873–80. [PubMed: 11731466]

Sive, H.; Grainger, R.; Harland, R. Early development of [i]Xenopus[/i] laevis : a laboratory manual. Cold Spring Harbor Laboratory Press; Cold Spring Harbor, N.Y.: 2000.

Sparrow DB, Jen WC, Kotecha S, Towers N, Kintner C, Mohun TJ. Thylacine 1 is expressed segmentally within the paraxial mesoderm of the [i]Xenopus[/i] embryo and interacts with the Notch pathway. Development. 1998; 125:2041–51. [PubMed: 9570769]

Sparrow DB, Latinkic B, Mohun TJ. A simplified method of generating transgenic [i]Xenopus[/i]. Nucleic Acids Res. 2000; 28:E12. [PubMed: 10648800]

Takahashi Y, Inoue T, Gossler A, Saga Y. Feedback loops comprising Dll1, Dll3 and Mesp2, and differential involvement of Psen1 are essential for rostrocaudal patterning of somites. Development. 2003; 130:4259–68. [PubMed: 12900443]

Takahashi Y, Kitajima S, Inoue T, Kanno J, Saga Y. Differential contributions of Mesp1 and Mesp2 to the epithelialization and rostro-caudal patterning of somites. Development. 2005; 132:787–96. [PubMed: 15677726]

Takahashi Y, Yasuhiko Y, Kitajima S, Kanno J, Saga Y. Appropriate suppression of Notch signaling by Mesp factors is essential for stripe pattern formation leading to segment boundary formation. Dev Biol. 2007; 304:593–603. [PubMed: 17306789]

Terasaki H, Murakami R, Yasuhiko Y, Shin IT, Kohara Y, Saga Y, Takeda H. Transgenic analysis of the medaka mesp-b enhancer in somitogenesis. Dev Growth Differ. 2006; 48:153–68. [PubMed: 16573733]

Turner DL, Weintraub H. Expression of achaete-scute homolog 3 in [i]Xenopus[/i] embryos converts ectodermal cells to a neural fate. Genes Dev. 1994; 8:1434–47. [PubMed: 7926743]

Vermot J, Gallego Llamas J, Fraulob V, Niederreither K, Chambon P, Dolle P. Retinoic acid controls the bilateral symmetry of somite formation in the mouse embryo. Science. 2005; 308:563–6. [PubMed: 15731404]

Vermot J, Pourquie O. Retinoic acid coordinates somitogenesis and left-right patterning in vertebrate embryos. Nature. 2005; 435:215–20. [PubMed: 15889094]

Westerfield, M. The Zebrafish Book: A guide for the laboratory use of zebrafish (Danio rerio). University of Oregon Press; Eugene, OR.: 2000.

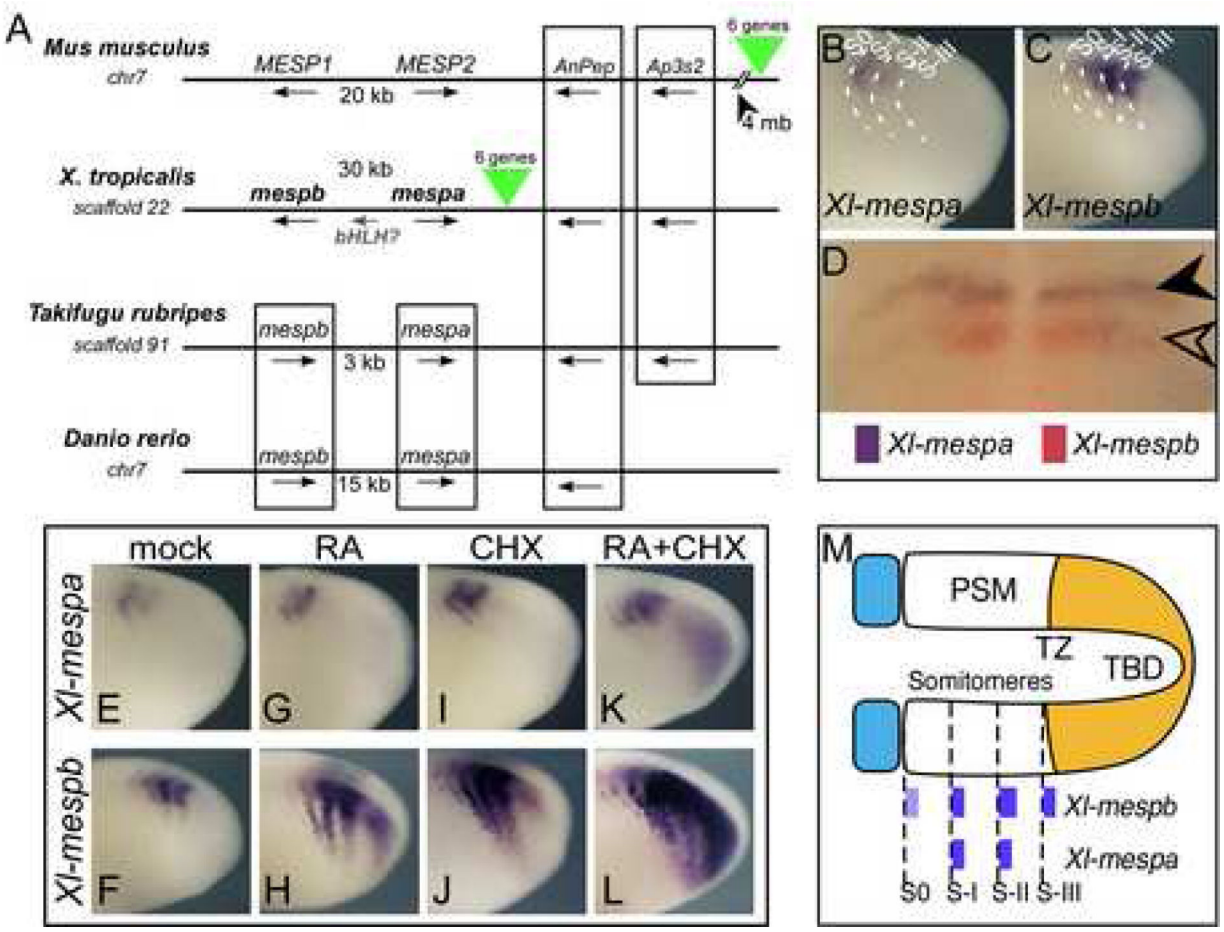

Figure 1.

Mesp genes in *Xenopus*. **(A) G**enomic organization of the *Mesp* genes. Shown are syntenic genomic regions from mouse, *Xenopus tropicalis*, *Takifugu rubripes*, and *Danio rerio*. Chromosome number is given when available, otherwise, scaffold number is indicated. Boxing indicates synteny of genes. *X. tropicalis* genes ENSXETG00000017725 and ENSXETG00000027628 are designated as *mespb* and *mespa* respectively. Green triangles indicate a syntenic block of 6 genes that are conserved between *X. tropicalis* and mouse, but in frog this block is between *mespa* and the *AnPep* gene, while in mouse the block is located 4 megabases (mb) away. **(B-C)** Expression of *Xl-mespa* and *Xl-mespb* in the PSM of *X. laevis* embryos by whole mount *in situ* hybridization. Dotted lines indicate approximate locations of somitomere boundaries. **(D)** Double *in situ* hybridization with *Xl-mespb* (red) and *Xl-mespa* (purple). **(E-L)** Shown is the expression of *Xenopus Mesp* genes after treatment with CHX and RA, as indicated. Treatment was for 1.5 h at RT prior to fixation. **(M)** Schematic representation of the PSM showing the relative locations of the somitomeres, transition zone (TZ), and tailbud (TBD) with *Xenopus Mesp* expression patterns indicated. Anterior is to the left in all panels.

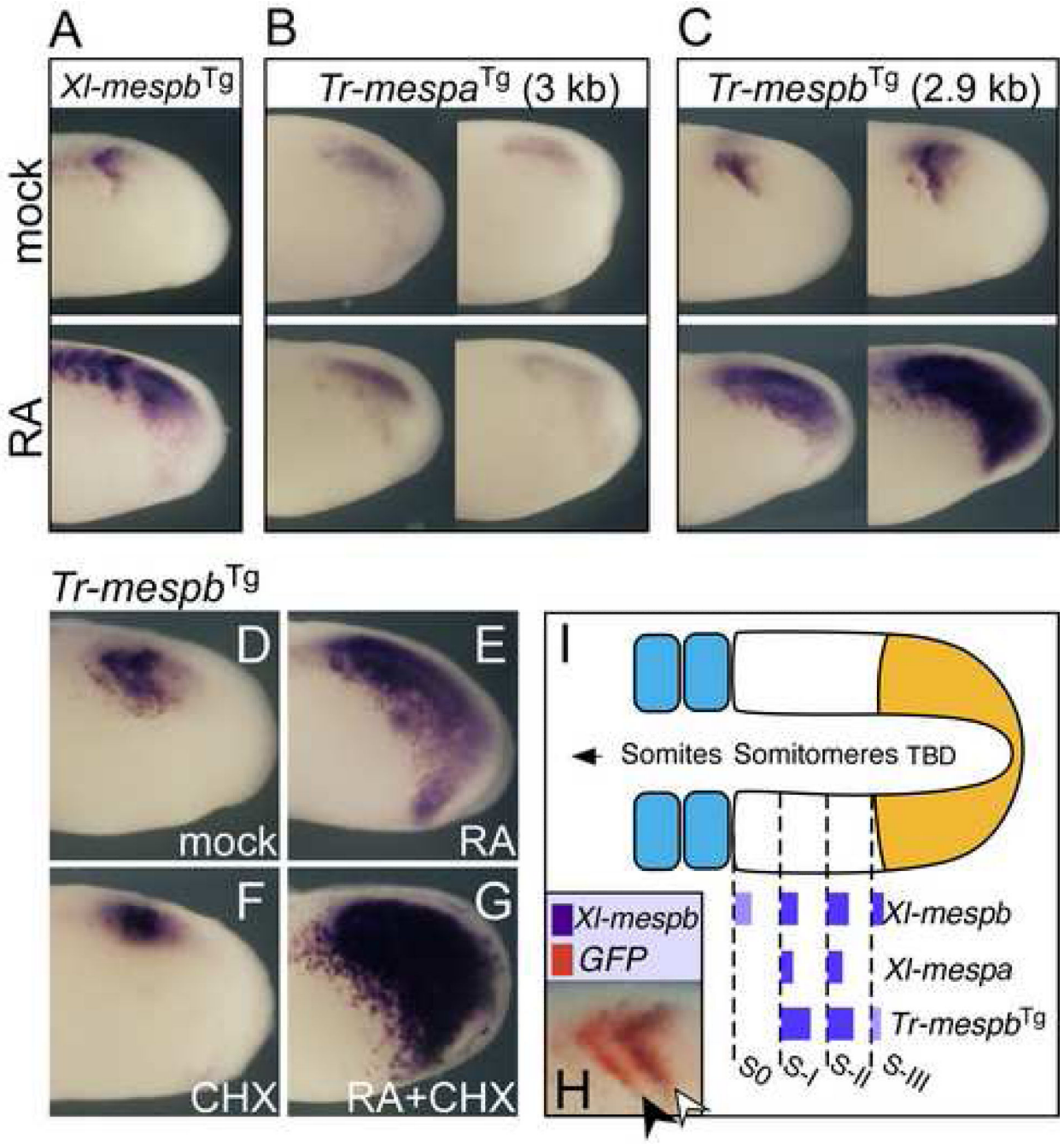

Figure 2.

The Fugu *Mesp* gene, *Tr-mespb*, responds to segmental patterning cues in *X. laevis* embryos. **(A-C)** Shown are *in situ* hybridizations for *GFP* reporter RNA in *X. laevis* embryos transgenic for *Xl-mespb*, *Tr-mespa* or *Tr-mespb* driving GFP. Transgenic embryos in lower panels were treated with RA 1.5 hours at RT prior to fixation. For *Tr-mesp* transgenes, two different embryos in each condition are shown. **(D-G)** The *Tr-mespb* transgene is strongly induced by RA alone and in the presence of CHX. **(H)** Double-label *in situ* hybridization for *Xl-mespb* (purple) and *GFP* reporter (red) RNA in *Tr-mespb* transgenic embryos. **(I)**

Schematic of PSM showing relative locations of transgenic *Tr-mespb* expression relative to the endogenous *Xenopus Mesp* genes. Anterior is to the left.

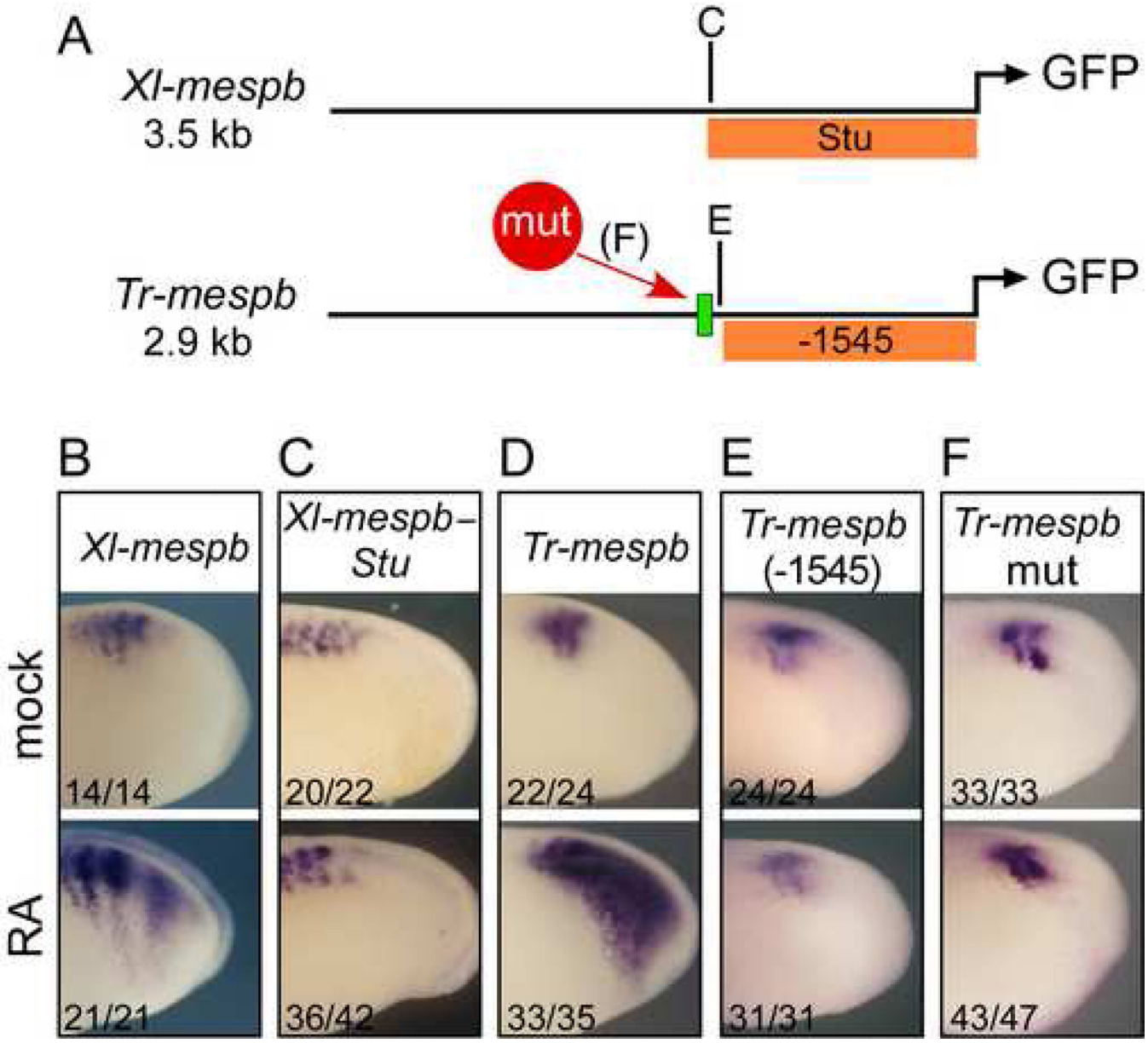

Figure 3.

The RA response element is arranged similarly in the *Tr-mespb* and *Xl-mespb* genes. **(A)**: Schematic diagram of transgene constructs with locations of truncation points and βRE (green box). The portion of *Tr-mespb* or *Xl-mespb* regulatory sequences contained in truncated constructs is indicated with orange bars. **(B-F)** *X. laevis* embryos transgenic for the indicated construct were untreated (top panels) or treated with RA (bottom panels) for two hrs at RT and stained for *GFP* reporter expression using whole-mount *in situ* hybridization. Numbers given are (# with phenotype shown)/(# expressing GFP). Anterior is to the left.

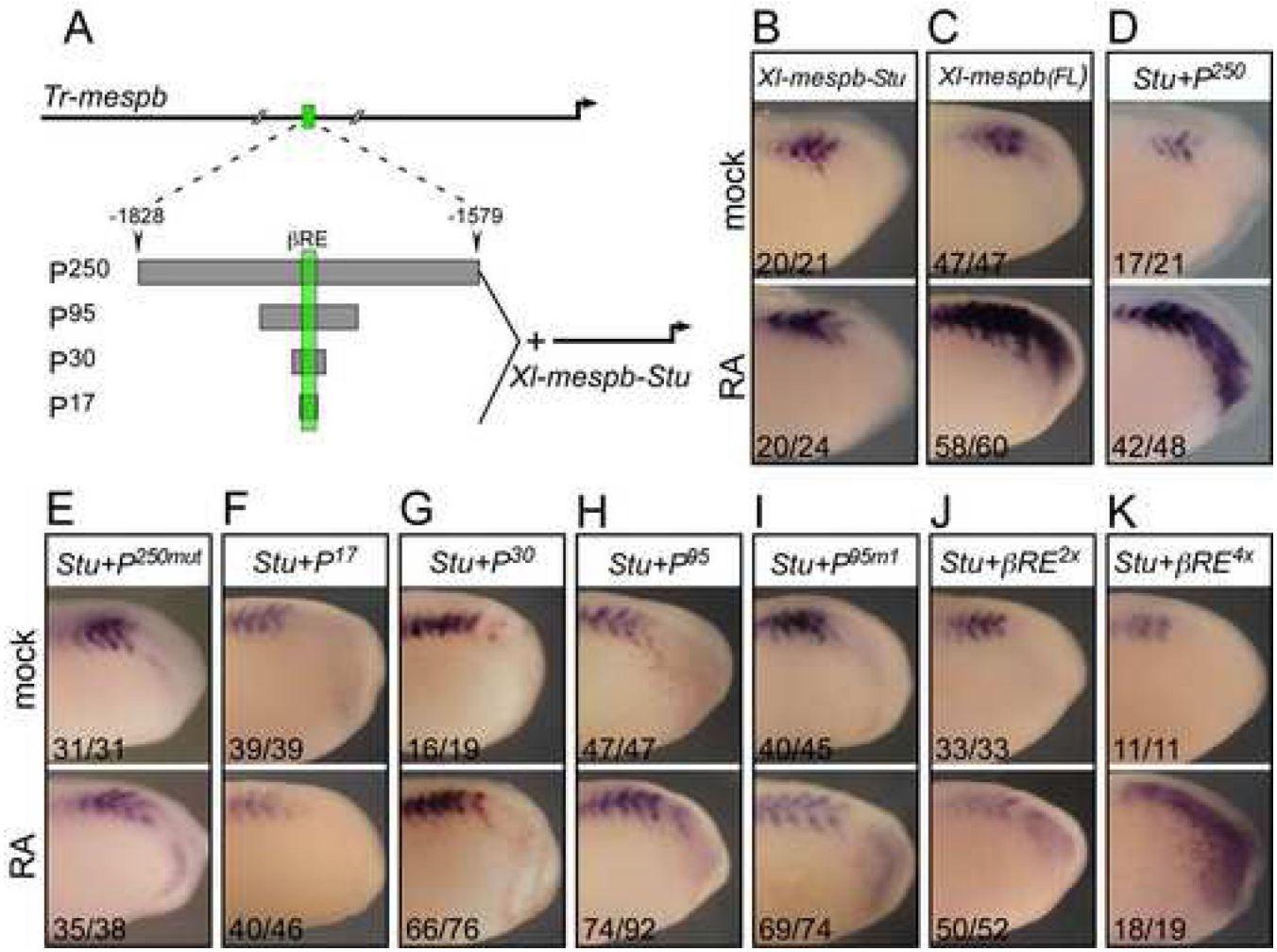

Figure 4.

The RA response element in *Tr-mespb*. **(A)** Diagram showing the portions of the *Tr-mespb* regulatory sequences surrounding the RARE (green box) that were appended to the 5′ end of the *Xenopus* stripe enhancer (*Xl-mespb-Stu*). **(B-K)** *Xenopus* embryos transgenic for the indicated constructs were untreated (top panels) or treated (bottom panels) with RA for two hrs at RT and stained for *GFP* expression using whole-mount *in situ* hybridization. Numbers given are (# with phenotype shown)/(# expressing GFP). Anterior is to the left in all panels.

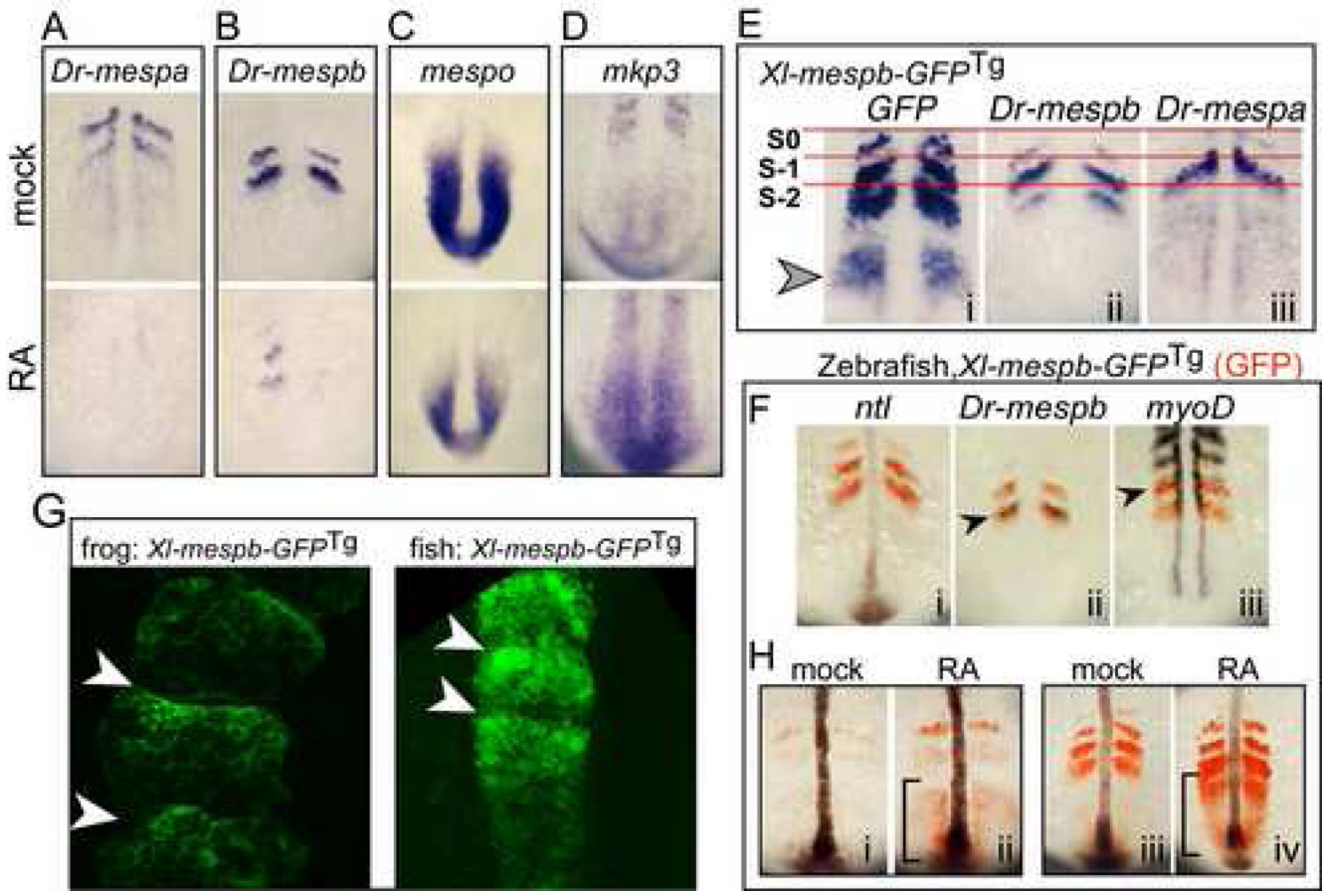

Figure 5.

Zebrafish *Mesp* genes respond differently to RA treatment. **(A-D)** Zebrafish embryos treated with carrier control (DMSO; top panels) or with RA (lower panels) for 3 hours and then stained for the expression of the indicated gene: A, *Dr-mespa*; B, *Dr-mespb*; C, *mespo*; D, *mkp3*. **(E)** Zebrafish embryos transgenic for *Xl-mespb-GFP* were stained for *GFP* RNA (i), *Dr-mespb* RNA (ii) or *Dr-mespa* RNA expression (iii) an aligned according to the first somite. **(F)** Double-label *in situs* on zebrafish embryos transgenic for *XMespβ–GFP* with *GFP* (red) and the gene indicated (purple) to localize the *GFP* expression pattern. **(G)**. *X. laevis* (left panel) and zebrafish embryos (right panel) transgenic for the full-length *Xl-mespb-GFP* were imaged by confocal microscopy. Shown is a region containing newly formed somites, and where somitic boundaries are marked with arrowheads **(H)** Zebrafish embryos transgenic for *Xl-mespb-GFP* were treated with RA at the 6 somite stage (i,ii) or 12 somite stage (iii, iv) and stained for *GFP* RNA (red) and for *no tail (ntl)* in purple to mark the notochord. Brackets mark the tailbud domain. Anterior is oriented up in all panels.

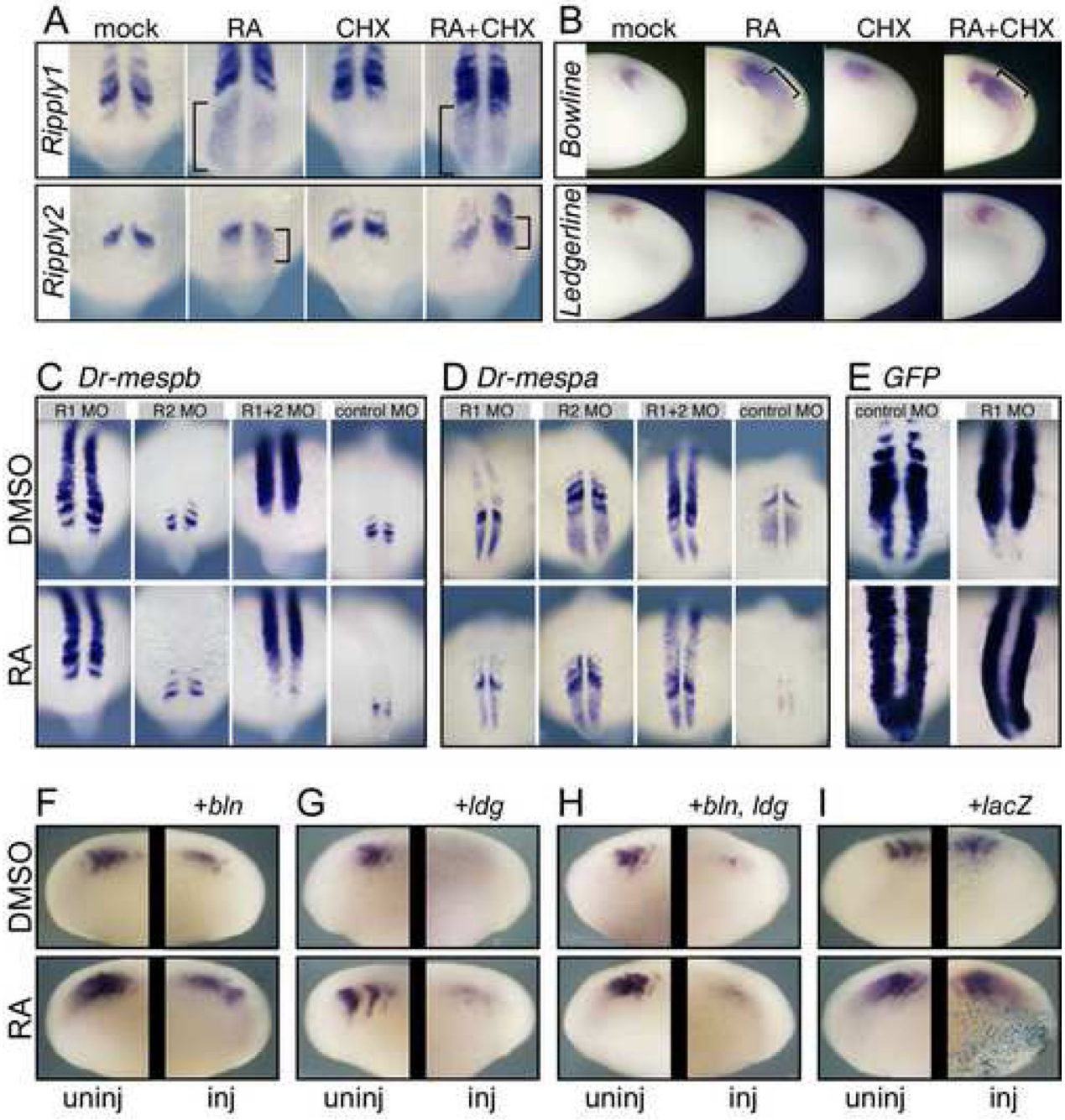

Figure 6.

Ripply genes modulate the RA response of *Mesp* genes. **(A)** Zebrafish embryos treated for 2 hours with RA and/or CHX as indicated and stained for the expression *Ripply1* (top row) or *Ripply2* (bottom row). Anterior is oriented up for zebrafish embryos. **(B)** *Xenopus* embryos treated for 1.5 hours with RA and/or CHX as indicated and stained for the expression of *bowline* (top row) or *ledgerline* (bottom row). Anterior is oriented to the left for frog embryos. **(C - E)** Zebrafish embryos injected with the indicated morpholino: R1 = anti-*Ripply1*; R2 = anti-*Ripply2*; R1+2 = both morpholinos. Injected embryos were treated for 4

hours with DMSO (carrier control) or with RA, and then stained for expression of C: *mespb*; D, *mespa*; or E, *GFP*. Anterior is up in all zebrafish panels. **(F-I)** *Xenopus* embryos injected with *bowline* (*bln*, F), *ledgerline* (*ldg*, G), both *bln* and *ldg* (H), or *lacZ* RNAs (I). Embryos were treated with DMSO or RA (top and bottom, respectively) and stained for localization of *XMespβ* transcripts. Within each boxed area, the two sides of a single embryo are shown. The uninjected side serves as an internal control and is always shown on the left side of the box.